Research Article | DOI: 10.5281/zenodo.14511893
www.jnanosam.com

NANOSAM
Journal of NanoScience in Advanced Materials

# The Nano-Sized h-BN Addition into $MgB_2$/Fe Superconducting Wires

**Fırat Karaboğa[1#], Hakan Yetiş[2] and İbrahim Belenli[2]**

**This paper reports on the effect of hexagonal boron nitride (h-BN) addition on the superconducting properties of in-situ iron (Fe) sheathed $MgB_2$ bare and added wire samples (Φ=1.15 mm and 1.25 mm, respectively). The structural, electrical, mechanical and transport properties of $MgB_2$ with 1 wt% h-BN addition compared to pure $MgB_2$ wires were investigated for five different annealing temperatures. The results showed that the addition of nano-sized h-BN did not significantly affect the critical transition temperature for all wire samples, but relatively improved the wire uniformity, which contributed to the conduction properties of the wires.**

## 1. Introduction

Since the discovery of magnesium diboride ($MgB_2$) in 2001 [1] as a superconductor with the highest critical transition temperature among conventional metallic superconductors, numerous researchers have focused on enhancing its mechanical, physical, and electrical properties through various methods, such as heat treatment, the use of additives, substitutions, doping, irradiation, and different types of raw materials for synthesis [2-12]. $MgB_2$ has gained significant interest for applications including magnetic resonance imaging (MRI), superconducting power cables, fault current limiters (FCLs), and superconducting generators and motors [13-19]. However, $MgB_2$ conductor technology still requires substantial advancements to enable the commercial use of $MgB_2$ wires and tapes in MRI superconducting magnets. Ongoing fundamental studies aim to address these challenges and scale up production. Improving $MgB_2$ conductor technology necessitates alternative production techniques or the introduction of new additives to enhance its transport properties further. By increasing the operational temperature, thanks to $MgB_2$'s high transport current at 10–20 K (in liquid hydrogen), its simple chemical composition, low density, minimal anisotropy, and cost-effectiveness, the overall operating cost of superconducting devices can be reduced [20,21]. Nonetheless, producing single-phase $MgB_2$ is challenging due to the complex reactions involving phases such as $MgB_4$, $MgB_6$, $MgB_7$, $MgB_{12}$, and MgO during the manufacturing process [22-27]. Nanoparticles have been favored as additives for improving critical parameters like critical current density ($J_c$), upper critical field ($H_{c2}$), and homogeneity. Hexagonal boron nitride (h-BN) and carbon-based materials, [28-31] known for their ability to enhance mechanical, thermal, and electrical properties, have emerged as promising candidates, with h-BN offering stability at high temperatures in air [32-35]. Depending on the required properties for specific applications, $MgB_2$ samples are needed in different forms, such as bulk, film, or wire [36]. Various factors, including the size and purity of components, annealing processes, oxidation, low mass density, and grain connectivity, contribute to the challenges mentioned. Among these, the most critical parameter is the critical current density, as it is closely tied to well-connected grains and uniformly distributed pinning centers in numerous applications.

This study comprehensively investigated the effects of lubrication during the cold drawing process and the addition of chemically stable, nano-sized h-BN on the superconducting properties of $MgB_2$/Fe wires. It was believed that exploring the

[1]*Department of Medical Services and Techniques, Bolu Abant İzzet Baysal of University, 14300, Bolu, Türkiye,* [2]*Department of Physics, Faculty of Art and Science, Bolu Abant İzzet Baysal of University, 14300, Bolu, Türkiye*

*#Corresponding author: karabogafirat@gmail.com*

*Keywords: $MgB_2$ wire; h-BN addition; phase formation; Impurities.*

Received: 18 October 2024 | Accepted: 05 November 2024 | Published online: 25 December 2024

NANOSAM
Journal of NanoScience in Advanced Materials

impact of h-BN as a nano-additive could provide valuable insights for advancing the use of $MgB_2$ materials in practical superconducting devices.

## 2. Results and Discussion

Figure 1 shows the resistivity vs. temperature ($\rho - T$) curves of the h-BN added and pure $MgB_2$ wires annealed at various temperatures. It seems that the critical temperature ($T_c$) does not change much with increasing annealing temperature for both h-BN added and pure wires. The $T_c$ is between 36.35 and 37.55 K as shown in Table 1 and the lowest $T_c$ value belongs to the h-BN added wire annealed at 900 ˚C. It is also observed that there is an increase of approximately 2 μΩ cm in the normal state resistivity of pure wires compared to h-BN added wires. However, this increase observed in both doped and pure wires annealed above 800 ˚C is more related to the increase in heat treatment temperature rather than the h-BN addition. It is also seen that sample 1 does not follow this systematic behavior. The highest resistivity value measured in sample 1 may be due to micro deformations occurring in the current transfer region.

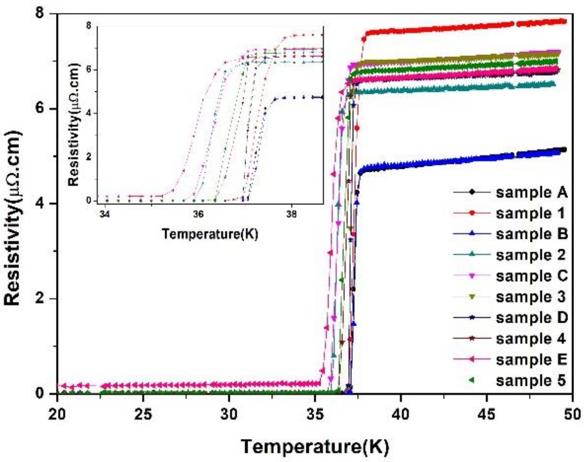


**Figure 1.** Resistivity vs temperature ($\rho$-$T$) curves for the studied Fe/$MgB_2$ wires annealed at different temperatures. Inset belongs to the magnified ($\rho$-$T$) curve.

Figures 2a–2b show the results of transport I–V measurements performed for h-BN added and pure wire samples at 36 K, a temperature very close to the $T_c$ of the wires, in the absence of an external magnetic field. In Fig. 2a, sample B and sample D wire samples having the highest $T_c$ values are capable of transporting 1 A at 36 K. However, h-BN added wires do not have $I_c$ values that change systematically with the change in annealing temperature, suggesting that the wire samples have some superconducting core differences that affect the $I_c$. A similar behavior is also present in pure wires as seen in Figure 2b, but I-V measurements also show that the effect of non-uniformities on transport properties of the pure wires is more pronounced. Considering these results, the lubricant properties of 12 nm h-BN nano particles seem to contribute to some extent to the core uniformity during the wire drawing process.

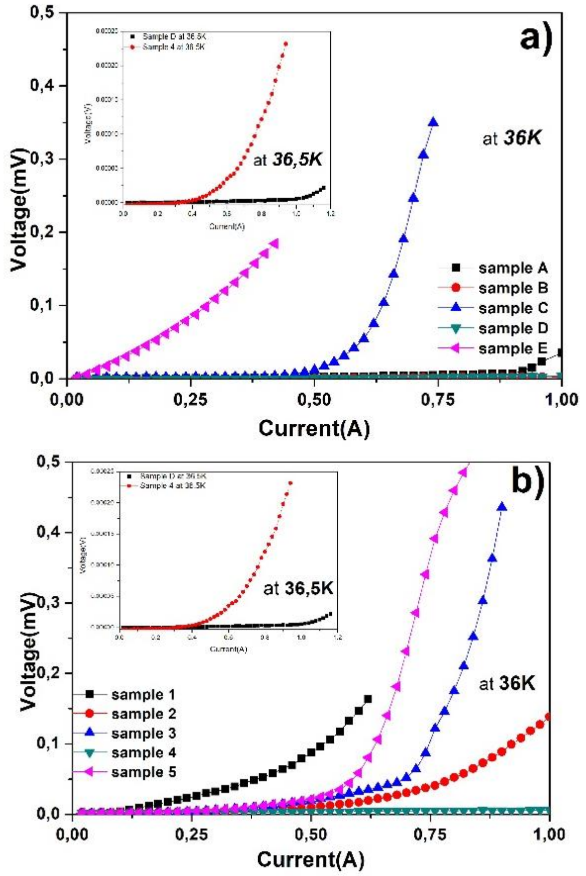


**Figure 2.** Transport current curve of h-BN added a) and pure b) samples for various temperatures. The insets show the I – V curves for sample D and sample 4 at 36.5 K.

Figure 3 shows the relationship between the $I_c$ values obtained from the I-V measurements at 34 and 36 K and the heat treatment temperature. As mentioned above, the h-BN added wires can exhibit relatively more systematic behavior compared to the pure wires. Heat treatment at 900 ˚C for both types of wire samples adversely affects the transport properties of the wires. Considering that h-BN is stable against decomposition at temperatures up to 900 ˚C in air [37], it seems that high annealing temperatures may cause the formation of more oxide phases in the core region.

Figure 4 shows the microhardness values of h-BN added and pure wire samples taken from the core region of the wires after cross-sectional polishing. It is observed that microhardness values are around 1 GPa for the h-BN wires and 1.1 GPa for pure wires,

**Table 1.** The onset and offset values of the critical transition temperatures for undoped (b) and 1% wt. h-BN doped $MgB_2$ samples (a). All data were extracted from the $\rho$-$T$ curves given in Figure 1.

| h-BN added $MgB_2$ wires | $T_c$ (K) | $\Delta T$ (K) | $\rho$ (μΩ.cm) (300K) | $\rho$ (μΩ.cm) (40K) | RRR ($\rho_{300K}/\rho_{40K}$) | $A_F$ ($\Delta\rho_{ideal}/\Delta\rho$) |
|---|---|---|---|---|---|---|
| **Sample A** | 37.07 | 0.5742 | 17.54 | 4.791 | 3.663 | 0.5735 |
| **Sample B** | 37.48 | 0.5641 | 16.82 | 4.791 | 3.512 | 0.6073 |
| **Sample C** | 37.02 | 1.273 | 21.59 | 6.993 | 3.095 | 0.5012 |
| **Sample D** | 37.55 | 0.8043 | 19.52 | 6.652 | 2.934 | 0.5676 |
| **Sample E** | 36.35 | 1.579 | 21.07 | 6.652 | 3.172 | 0.5061 |
| **Pure $MgB_2$ wires** | | | | | | |
| **Sample 1** | 37.20 | 0.9421 | 22.01 | 7.631 | 2.882 | 0.508 |
| **Sample 2** | 37.29 | 0.5072 | 20.04 | 6.383 | 3.144 | 0.535 |
| **Sample 3** | 37.30 | 0.6221 | 20.24 | 7.004 | 2.893 | 0.552 |
| **Sample 4** | 37.20 | 0.5644 | 20.14 | 6.642 | 3.031 | 0.541 |
| **Sample 5** | 37.26 | 0.4072 | 20.35 | 6.811 | 2.992 | 0.539 |

but the pure samples have relatively high and unstable values in comparison to that of h-BN added wires. This analysis is again consistent with the arguments showing that h-BN samples have better core uniformity than that of undoped wires. Microhardness values around 1 GPa support the fact that similar amounts of $MgB_2$ phase formation occur in the wires at all heat treatment temperatures. Additionally, it can be said that the h-BN added wires are more drawable than undoped ones without breakages during cold drawing process due to lubricant property of h-BN in literature [38].

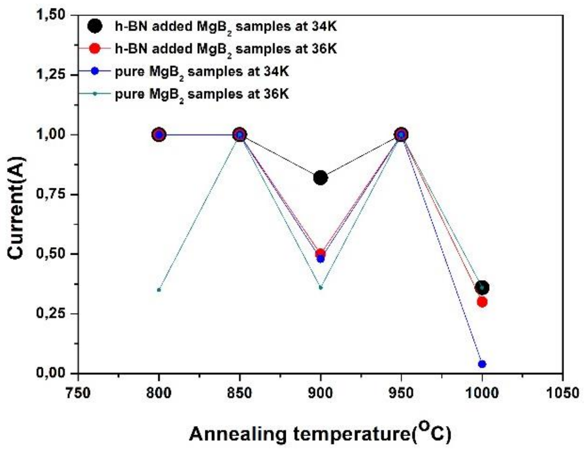


**Figure 3.** Transport current values of h-BN added and pure samples for various annealing temperatures.

The structural properties of 12 nm h-BN added, and pure wires are given in Figure 5. Ag peaks belong to silver holder used for XRD measurement of very small amount of $MgB_2$ powder obtained after removing of Fe sheath in the wire. The lattice parameters calculated from the X-ray diffraction patterns of the wire are given in Table 2. It is seen that the MgO peak is more pronounced in the wires annealed at 900 ˚C. This result explains the poor transport properties in the samples annealed at 900 ˚C. The formation of magnesium oxide negatively affected the connectivity [39]. The lattice parameters are close to each other in pure and h-BN doped wires, which is an indication that the added h-BN nanoparticles accumulate in the intergranular regions. It can be said that there is no peak indicating the formation of phases such as $MgB_4$, which is one of the impurity phases for superconducting $MgB_2$ phase, in wires annealed at high temperatures [40].

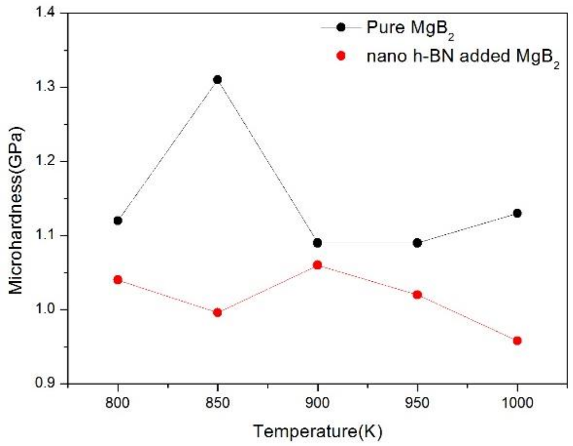


**Figure 4.** The microhardness values of the wires depending on sintering temperature.

## 3. Conclusion

We studied the effect of adding h-BN nano particles into in-situ $MgB_2$/Fe wires as a function of annealing temperature. The results showed that h-BN nano particles did not directly improve the superconducting and transport properties of $MgB_2$/Fe wires. However, it was observed that lubricant property of h-BN contributes to the core uniformity of the $MgB_2$ wires during cold drawing.

**Table 2.** Crystallity parameters for the studied $MgB_2$ samples. All data extracted from curves in Figure 5.

| h-BN added $MgB_2$ samples | a lattice(Å) | c lattice (Å) | Grain size (Å) | FWHM | Strain |
|---|---|---|---|---|---|
| **Sample A** | 3.113 | 3.532 | 29.66 | 0.3311 | 0.2115 |
| **Sample B** | 3.101 | 3.526 | 26.42 | 0.3607 | 0.2293 |
| **Sample C** | 3.095 | 3.528 | 35.43 | 0.2838 | 0.1803 |
| **Sample D** | 3.095 | 3.529 | 33.64 | 0.3003 | 0.1911 |
| **Sample E** | 3.093 | 3.523 | 37.27 | 0.2808 | 0.1788 |
| **Pure $MgB_2$ samples** | | | | | |
| **Sample 1** | 3.092 | 3.523 | 26.46 | 0.3599 | 0.2286 |
| **Sample 2** | 3.101 | 3.531 | 28.44 | 0.3411 | 0.2173 |
| **Sample 3** | 3.102 | 3.534 | 30.78 | 0.3203 | 0.2041 |
| **Sample 4** | 3.097 | 3.531 | 30.78 | 0.3217 | 0.2045 |
| **Sample 5** | 3.092 | 3.524 | 33.37 | 0.2984 | 0.1898 |

The h-BN nanoparticles have a high decomposition temperature of above 900 ˚C; it is observed from X-ray analysis that the h-BN particles were mostly located at intergranular region. In Figure5, the peaks indicated h-BN could not be directly seen due to the resolution of XRD measurement system and very small amount of h-BN addition (1%). The pinning properties of h-BN particles will be considered as future work to study h-BN added $MgB_2$ wires under external magnetic field in detail.

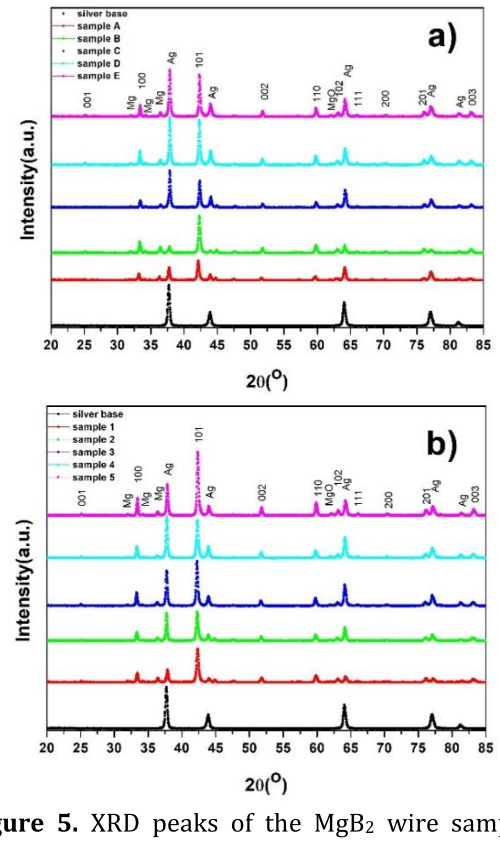


**Figure 5.** XRD peaks of the $MgB_2$ wire samples which are a) doped and b) undoped. Black line belongs to silver holder base.

## Method

A high purity atomized spherical Mg powder (99.0% - 100-200 mesh) and elemental amorphous boron (95-97% pure) bought by Pavezyum Company were weighed and mixed in 1:2 ratio as stoichiometric for preparation of first mixture. Other powder was also obtained by adding boron nitride 1% of Mg and Boron mixture in 1:2 ratio as weight. After that, two iron tubes were cut 20 cm in length. The outer and inner diameter of the used Fe tube are 12mm and 9mm. They were cleaned in alcohol with an ultrasonic system. Then, the Fe tubes were filled separately with same weight powder by using the obtained mixtures. In both preparation processes, the aluminum foil was pressed as stopper in both sides of iron tube. The prepared two samples were drawn from 12 mm to ~1.15 mm in outer diameter. The diameter reduction and intermediate annealing processes of pure and 12 nm h-BN 1% added $MgB_2$ wires were same for comparison easily to each other. The produced wires were cut 100 mm in length and put into controllable tube furnace for an annealing process. The annealing was performed at several temperatures such as 700, 750, 800, 850 and 900 ˚C for 1 hour under 5 bar high purity argon gas with 5°C/min heating and cooling rates. The obtained superconducting wires were named sample A (700 ˚C), B (750 ˚C), C (800 ˚C), D (850 ˚C), and E (900 ˚C) for 12 nm h-BN added wires and sample 1 (700 ˚C), 2 (750 ˚C), 3 (800 ˚C), 4 (850 ˚C), and 5 (900 ˚C) for undoped wires.

The crystal structure, grain size, phase formation and lattice parameters of the wires were analyzed by using Rigaku-Multiflex X-ray diffractometer (XRD) consisting of CuKα radiation (λ = 1.5418 Å) in the range of 10o and 90o with a scan speed of 5 ˚/min in ambient conditions. The DC electrical measurements such as resistivity versus temperature ($\rho$-$T$) and

NANOSAM
Journal of NanoScience in Advanced Materials

transport critical current ($I_c$) of the wires were performed by using standard four probe technique in a closed-cycle cryostat system (CRYO Industries). Temperature dependent resistivity measurements were carried out from 20 K to 50 K by applying 50 mA DC current. Critical current test was performed at constant temperature close to critical transition temperature ($T_c$) by applying maximum current of 1 A. The programmable Keithley 2182A and Keithley 220 were used as nano-voltmeter and current source, respectively. Micro-hardness values were taken from the polished cross-sections of these wires by means of SHIMADZU HVM-2 micro-hardness tester. The used load was 2.940 N for 10 seconds with 0.1 μm accuracy.

## Acknowledgements

I want to thank for facility of laboratory of the late Prof. Dr. Çetin BOZKURT and supporting Dr. Muhammed ÖZ.

## Conflicts of Interest

The authors stated that did not have conflict of interests.

## Author Contributions

All authors contributed to the design and concept of the study. All authors contributed to the preparation of sample production, characterization, arrangement of the draft version of the manuscript, and the final version of the article. All authors read and approved the final version of the manuscript.

## Data Availability Statement

The datasets generated during and/or analysed during the current study are available from the corresponding author on reasonable request.

## Reference

**[1]** Nagamatsu, J., Nakagawa, N., Muranaka, T., Zenitani, Y., Akimitsu, J., Superconductivity at 39 K in magnesium diboride, Nature **410**, 63 (2001).

**[2]** Da Silva, L.B.S., Serrano, G., Serquis, A., Metzner, V.C.V., Rodrigues, D., Study of TaB2and SiC additions on the properties of MgB2superconducting bulks, Superconductor Science and Technology **28**, 025008 (2015).

**[3]** Erdem, O., and Yanmaz, E., Effect of Er doping on the superconducting properties of porous MgB2, Bulletin of Materials Science **38**, 89 (2015).

**[4]** Novosel, N., Galic, S., Pajic, D., Zadro, K., Babic, E., Enhancing Superconducting Proprties of MgB2 by Addition of Magnetic Particles, Journal of Superconductivity and Novel Magnetism **28**, 425 (2015).

**[5]** Qin, F., Cai, Q., Chen, H., Partial dissolution of MgO and the effect on critical current density in urea-doped MgB2 bulks, Journal of Alloys and Compounds **633**, 201 (2015).

**[6]** Shah, M.S., Shahabuddin, M., Parakkandy, J.M., Alzayed, N.S., Madhar, N.A., Batoo, K.M., Effects of High Pressure Using Cold Isostatic Press on the Physical Properties of Nano-SiC-Doped MgB2, Journal of Superconductivity and Novel Magnetism **28**, 481 (2015).

**[7]** Wang, D.L., Zhang, H.T., Zhang, X.P., Tang, S.P., Ma, Y.W., Oguro, H., Awaji, S., Watanabe, K., Effects of three different homemade nanocarbons doping on the superconducting properties of MgB2 tapes, Physica C Superconductivity **508**, 49 (2015).

**[8]** Yang, F., Li, S.Q., Yan, G., Feng, J.Q., Xiong, X.M., Zhang, S.N., Wang, Q.Y., Liu, G.Q., Pang, Y.C., Zou, H.F., Li, C.S., Feng, Y., Improved superconducting properties in Ti-doped MgB2 prepared by two-step reaction method and high-energy ball milling, Journal of Alloys and Compounds **622**, 714 (2015).

**[9]** Yilmazlar, M., Terzioglu, C., Dogruer, M., Karaboga, F., Soylu, N., Zalaoglu, Y., Yildirim, G., Ozturk, O., Evaluation of Microstructural and Mechanical Properties of Ag-Diffused Bulk MgB2 Superconductors, J Supercond Nov Magn. **27**, 77 (2014).

**[10]** Q.Z. Shi, Z.S. Yan, Effect of nano-Al2O3 doping on formation and superconductivity of bulk MgB2, Journal of Materials Science: Materials in Electronics **21**, 656 (2010).

**[11]** Vinod, K., Varghese, N., Sundaresan, A., Syamaprasad, U., Highly enhanced in-field critical current density of MgB2 superconductor by combined addition of burned rice husk and nano Ho2O3, Solid State Sciences **12**, 610 (2010).

**[12]** Bhadauria, P.P.S., Gupta, A., Kishan, H., Narlikar, A.V., Effect of excess Mg and nano-additives on the superconducting properties of weakly connected bulk MgB2, Journal of Applied Physics **113**, 63908 (2013).

**[13]** Fracasso, M., Gomory, F., Solovyov, M., Gerbaldo, R., Ghigo, G., Laviano, F., Sparacio, S., Torsello, D., Gozzelino, L., Numerical study on flux-jump occurrence in a cup-shaped MgB2 bulk for magnetic shielding applications, Superconductor Science and Technology **36** (4), 044001(2023).

**[14]** Gao, Z., Santra, S., Amirkhanlou, S., Eardley, E., Wort, C., Grovenor, C.R., Speller, S.C., Microstructures and superconducting properties of MgB2 bulk samples processed by ultra-high pressure-assisted sintering, Journal of the European Ceramic Society **42** (16), 7481–7490 (2022).

**[15]** Durrell, J.H.,Towards high performance desktop NMR using bulk MgB2 superconductors, Superconductor Science and Technology **34**, 080502 (2021).

**[16]** Kambara, M., Babu, N.H., Sadki, E., Cooper, J., Minami, H., Cardwell, D., Campbell, A., Inoue, I., High intergranular critical currents in metallic MgB2 superconductor, Superconductor Science and Technology **14** (4) L5,(2001).

**[17]** Takano, Y., Takeya, H., Fujii, H., Kumakura, H., Hatano, T., Togano, K., Kito, H., Ihara, H., Superconducting properties of MgB2 bulk materials prepared by high-pressure sintering, Applied Physics Letters **78** (19) 2914–2916, (2001).

**[18]** Zhao, Y., Feng, Y., Cheng, C., Zhou, L., Wu, Y., Machi, T., Fudamoto, Y., Koshizuka, N., Murakami, M., High critical current density of MgB2 bulk superconductor doped with Ti and sintered at ambient pressure, Applied Physics Letters **79** (8) 1154–1156, (2001).

**[19]** Serquis, A., Zhu, Y., Peterson, E., Coulter, J., Peterson, D., Mueller, F., Effect of lattice strain and defects on the superconductivity of MgB2, Applied Physics Letters **79** (26) 4399–4401, (2001).

**[20]** Buzea, C., Yamashita, T., Review of the superconducting properties of MgB2, Supercond Sci Tech. **14**, R115 (2001).

**[21]** S. Zhou, Y. Zhang, A.V. Pan, S.X. Dou, K.C. Chung, Y.K. Kim, J.M. Yoo, Effects of sintering atmosphere on the superconductivity of MgB2, Superconductor Science and Technology **22**, 045018 (2009)

**[22]** Kolesnikov, N.N., Kulakov, M.P., Synthesis of MgB2 from elements, Physica C: Superconductivity **363**, 166 (2001)

**[23]** Zhang, Y., Zhou, S.H., Wang, X.L., Dou, S.X., Effect of addition of nanoparticle TiO2/SiO2 on the superconducting properties of MgB2, Physica C: Superconductivity **468**, 1383 (2008).

**[24]** Liu, D.B., Chen, M.F., Rauf, A., Cui, C.X., Tan, J.J, Preparation and characterization of copper matrix composites by reaction sintering of the Cu–Mg–B system, Journal of Alloys and Compounds **466**, 87 (2008).

**[25]** Prikhna, T., Gawalek, W., Eisterer, M., Weber, H.W., Noudem, J., Sokolovsky, V., Chaud, X., Moshchil, V., Karpets, M., Kovylaev, V., Borimskiy, A., Tkach, V., Kozyrev, A., Kuznietsov, R., Dellith, J., Shmidt, C., Basyuk, T., Litzkendorf, D., Karau, F., Dittrich, U., Tomsic, M., Superconductivity in multi-phase Mg-B-O compounds, Forschungsbereich Low Temperature Physics and Superconductivity **36**, 475 (2012).

**[26]** Schmitt, R., Glaser, J., Wenzel, T., Nickel, K.G., Meyer, H.J., A reactivity study in the Mg–B system reaching for an improved synthesis of pure MgB2, Physica C: Superconductivity **436**, 38 (2006).

**[27]** Wenzel, T., Nickel, K.G., Glaser, J., Meyer, H.-J., Eyidi, D., Eibl, O., Electron probe microanalysis of Mg-B compounds: Stoichiometry and heterogeneity of superconductors, Physica Status Solidi (A) **198**, 374 (2003).

**[28]** Badica, P., Aldica, G., Burdusel, M., Popa, S., Negrea, R.F., Enculescu, M., Pasuk, I., Miu, L., Significant enhancement of the critical current density for cubic BN addition into ex situ spark plasma sintered MgB2, Superconductor Science and Technology **27**, 095013 (2014).

**[29]** Su, X.C., Jiang, Q.G., Zuo, A.Y., Influence of Ball-Milling Treatment of B Original Powder on the Phase Formation and Critical Current Density of Graphite Doped MgB2, Journal of Low Temperature Physics **177**, 8 (2014).

**[30]** Solozenka, V.L., Turkevich, V.Z., Holzapfel, W.B., Refined Phase Diagram of Boron Nitride, The Journal of Physical Chemistry B **103**, 8137 (1999)

**[31]** Pan, X.F., Zhao, Y., Feng, Y., Yang, Y., Cheng, C.H., Effects of graphite doping on critical current density and microstructure of MgB2 bulks by an improved Mg-diffusion method, Physica C: Superconductivity **468**, 1169 (2008).

**[32]** Dou, S.X., Soltanian, S., Horvat, J., Wang, X.L., Zhou, S.H., Ionescu, M., Liu, H.K., Munroe, P., Tomsic, M., Enhancement of the critical current density and flux pinning of MgB2 superconductor by nanoparticle SiC doping, Applied Physics Letters **81**, 3419 (2002).

**[33]** Kovac, P., Husek, I., Melisek, T., Grovenor, C.R.M., Haigh, S., Jones, H., Improvement of the current carrying capability of ex situ MgB2 wires by normal particle additions, Superconductor Science and Technology **17**, 1225 (2004).

**[34]** Wang, C.C., Wang, C., Zeng, R., Dou, S.X., Intergrain connectivity of MgB2 ceramics studied by impedance analysis, Journal of Applied Physics **108**, 023901 (2010).

**[35]** Soltanian, S., Delfany, M., Wang, X.L., Qin, M.J., Liu, H.K., Dou, S.X., Effects of Nano-Sized BN Doping on the Phase Formation, Tc and Critical Current Density of MgB2 Superconductor, Journal of Metastable and Nanocrystalline Materials **23**, 113 (2005).

**[36]** Sharma, R.G., Practical magnesium diboride (MgB2) superconductor, Springer Series in Materials Science **214**, 277-312 (2021).

**[37]** Wong, T.L., Vallés, C., Nasser, A., Abeykoon, C., Effects of boron-nitride-based nanomaterials on the thermal properties of composite organic phase change materials: A state-of-the-art review, Renewable and Sustainable Energy Reviews **187**, 113730-113753 (2023).

**[38]** Karaboga, F., Yetis, H., Öz, M., Belenli, I., Effect of different-sized h-BN nanoparticles on some properties of MgB2 superconductors, Journal of Materials Science: Materials in Electronics **27**, 8512–8517 (2016).

**[39]** Singh, D.K., Tiwari, B., Jha, R., Kishan, H., Awana, V.P.S., Role of MgO impurity on the superconducting properties of MgB2, Physica C: Superconductivity and Its Applications **505**, 104-108 (2014).

**[40]** Cai, Q., Liu, Y., Ma, Z., Li, H., Yu, L., Variation of pinning mechanism and enhancement of critical current density in MgB2 bulk containing self-generated coherent MgB4 impurity, Applied Physics Letters **103**, 132601-132608 (2013).